

A Single-Phase To Three-Phase Power Conversion System with Parallel Rectifier and Series Inverter

CH.RAVALI¹ S. SAI KIRAN KUMAR² D. RAMESH³

¹PG Scholar, Dept of EEE(Power & Industrial Drives),Nova College Of Engineering & Technology, Hyderabad, TS, India.

² Associate Professor, Dept of EEE, Nova College Of Engineering & Technology, Hyderabad, TS, India

³ Associate Professor, Head of Dept (EEE), Nova College Of Engineering & Technology, Hyderabad, TS, India

ABSTRACT: This project presents a single-phase to three-phase power conversion system with parallel rectifier and series inverter to cope with single-phase to three-phase asymmetry. Such converter guarantees both reduction in the input current processed by rectifier circuit (due to the parallel connection) and reduction of the output voltage processed by each inverter (due to the series connection). It is worth mentioning that, in spite of proposing a topology with features not yet observed in the technical literature, this paper presents a comprehensive model of the proposed converter, modulation strategy, and a general comparison with the conventional configuration. In extension we proposed FUZZY controller and Simulated results are also presented.

Keywords: Rectifier, inverter, power conversion, pulse width modulation

I. INTRODUCTION

In the power distribution systems, the single-phase grid has been considered as an alternative for rural or remote areas, due to

its lower cost feature, especially when compared with the three-phase solution. In huge countries like Brazil, the single-phase grid is quite common due to the large area to be covered. On the other hand, loads connected in a three-phase arrangement present some advantages when compared to single phase loads. This is especially true in three-phase motor systems with variable-speed drives due to their constant torque characteristic. In this scenario, there is a need for single-phase to three-phase power conversion systems. The direct solutions for the single-phase to three-phase power converters are presented in Fig. 1 Fig. 1(b) shows a solution for single-phase to three-phase power conversion, in which all variables (e.g., input power factor and dc-link voltage) at input–output converter sides can be controlled, On the other hand, the configuration presented in Fig. 1 (a) represents a cheaper solution but without any control of the input current and dc-link voltage. In general terms, a single-phase to three-phase power conversion presents an

inherent asymmetry, i.e., constant power at the output-converter side (three-phase load) and pulsating power at the input-converter side (single-phase grid). The direct consequence of this asymmetry is the low frequency voltage oscillation observed in the dc-link capacitors, as well as the power switches of the rectifier and inverter operate with different voltage and current ratings. Normally, the three-phase

motor-rated voltage is higher than that furnished by the single-phase grid (considering the Brazilian voltages available, it is possible to identify: $v_{in} = 110\text{ V}$, $v_{out} = 220\text{ V}$, or $v_{in} = 220\text{ V}$, $v_{out} = 220\text{ V}$ - depending of the region), which means that the rectifier circuit must boost the grid voltage to guarantee the motor-rated voltage.

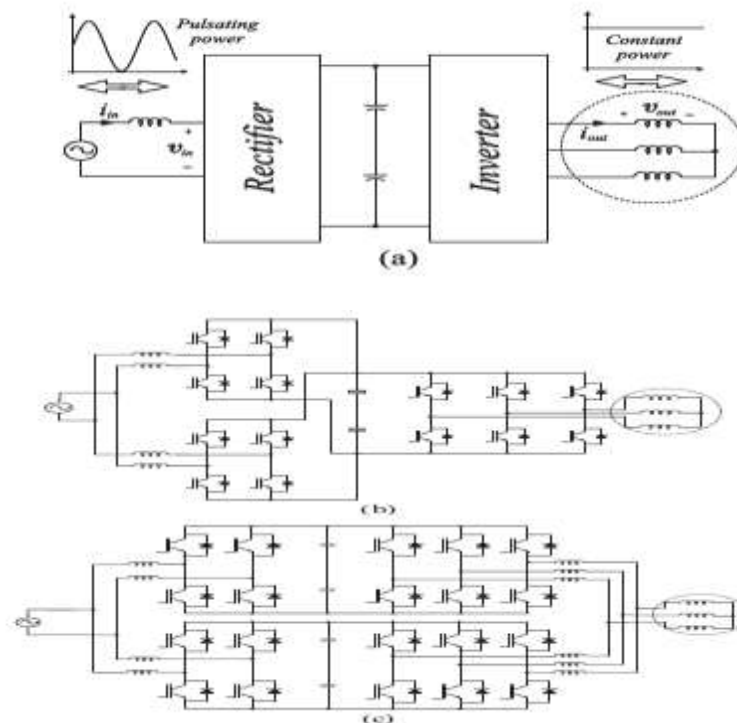


Fig. 1. Single-phase to three-phase power conversion. Type of power processed by rectifier and inverter circuits.

Furthermore, the current relation between input- and output-converter sides also implies in converter asymmetry, i.e., ($i_{in} > i_{out}$). Another important characteristic observed in the single-phase to three-phase power converters that also has been considered in this paper is the irregular distribution of power losses among the switches of the converter. It means that, for a 600 V 50A class of insulated gate bipolar transistor (IGBT),

63% of the total losses measured in the single-phase to three-phase converter is concentrated in the rectifier circuit, while the rest 37% is observed in the inverter circuit. With those numbers, it is possible to measure the stress by switch, which means that each rectifier switch is responsible for 15.7% of the total converter losses, while each inverter switch is responsible for only 6.1%. The loss per switch gives an

important parameter regarding the possibilities of failures in the power converters. Many configurations have been considered to deal with this asymmetry, as in in which a parallel rectifier circuit is considered to reduce the current processed by rectifier switches, as well as to improve the harmonic distortion, reliability, and efficiency at the input-converter side. With the same philosophy, Jacobin *et al*/proposes two

single-phase to three-phase ac–dc–ac converters paralleled [see Fig.], meaning improvements at input–output converter sides. To handle with the low-frequency voltage fluctuation observed in the dc-link voltage, Inhuman and Itch in and present a configuration with a specific control method for a single-phase to three-phase power converter with power decoupling function.

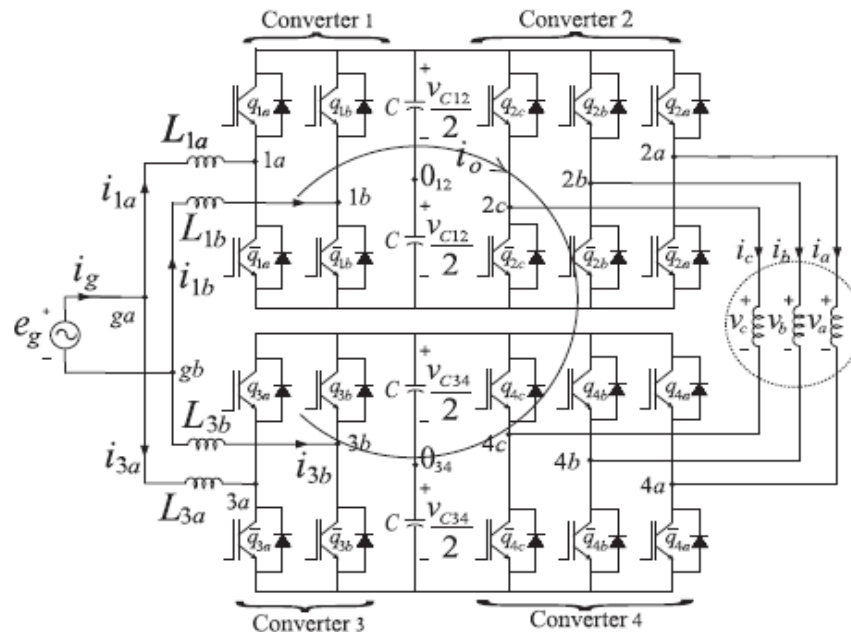


Fig.2. Proposed single-phase to three-phase conversion system.

Inverter (due to the series connection). It is worth mentioning that, in spite of proposing a topology with features not yet observed in the technical literature, this paper presents a comprehensive model of the proposed converter, modulation strategy, and a general comparison with the conventional configuration. Experimental results are used for the validation purpose.

III. MODELLING OF PROPOSED SYSTEM:

This section will present the model of the proposed configuration. Such a configuration is constituted by a single phase grid (e_g), one open-end three-phase motor, inductor filters (L_{1a} , L_{1b} , L_{3b} , and L_{3a}), converters 1, 2, 3, and 4, and two dc link capacitor banks (C_{12} and C_{34}). If the legs are substituted by pulsed voltage sources, the proposed converter can be modeled as in FIG.

A. Grid-Side Converter Model

:

$$e_g = r_{1a}i_{1a} + l_{1a} \frac{di_{1a}}{dt} - r_{1b}i_{1b} - l_{1b} \frac{di_{1b}}{dt} + v_1$$

$$e_g = r_{3a}i_{3a} + l_{3a} \frac{di_{3a}}{dt} - r_{3b}i_{3b} - l_{3b} \frac{di_{3b}}{dt} + v_3$$

$$i_g = i_{1a} + i_{3a}$$

$$v_1 = v_{1a012} - v_{1b012}$$

$$v_3 = v_{3a034} - v_{3b034}$$

where i_{1a} and i_{1b} are the input currents of the converter 1, i_{3a} and i_{3b} are the input currents of the converter 3, the symbols r and l represent the resistance and inductance of inductors L_{1a} , L_{1b} , L_{3a} , and L_{3b} . The voltages v_{1a012} and v_{1b012} are the pole voltages of the converter 1, while

From the system the following equations can be derived to converters 1 and 3 at the grid side

v_{3a034} and v_{3b034} are the pole voltages of the converter 3 and i_g is the grid current.

B. Machine-Side Converter Model

From the system the following equations can be derived to converters 2 and 4 at the machine side:

$$v_{ab} = v_{2a012} - v_{2b012} + v_{4b034} - v_{4a034}$$

$$v_{bc} = v_{2b012} - v_{2c012} + v_{4c034} - v_{4b034}$$

$$v_{ca} = v_{2c012} - v_{2a012} + v_{4a034} - v_{4c034}$$

where v_{2a012} , v_{2b012} , and v_{2c012} are the pole voltages of converter 2, v_{4a034} , v_{4b034} , and v_{4c034} are the pole voltages of converter 4, and $v_{ab} = v_a - v_b$, $v_{bc} = v_b - v_c$, and $v_{ca} = v_c$

– v_a are line-to-line voltages of the machine. For the voltage control of the motor, the following relations are obtained:

$$\begin{aligned} v_{2ab} &= v_{2a012} - v_{2b012} = \frac{v_{ab}}{2} \\ v_{2bc} &= v_{2b012} - v_{2c012} = \frac{v_{bc}}{2} \\ v_{2ca} &= v_{2c012} - v_{2a012} = \frac{v_{ca}}{2} \\ v_{4ab} &= v_{4a034} - v_{4b034} = -\frac{v_{ab}}{2} \\ v_{4bc} &= v_{4b034} - v_{4c034} = -\frac{v_{bc}}{2} \\ v_{4ca} &= v_{4c034} - v_{4a034} = -\frac{v_{ca}}{2} \end{aligned}$$

C. Three-Phase Motor Model

A typical three-phase machine has been used in this study. Selecting a fixed coordinate reference frame, the mathematical model that describes the

dynamic behavior of the three-phase induction motor is given by

$$\begin{aligned} \mathbf{v}_{sdq} &= r_s \mathbf{i}_{sdq} + \frac{d}{dt} \phi_{sdq} \\ \mathbf{v}_{rdq} &= r_r \mathbf{i}_{rdq} + \frac{d}{dt} \phi_{rdq} - j\omega_r \phi_{rdq} \\ \phi_{sdq} &= l_s \mathbf{i}_{sdq} + l_{sr} \mathbf{i}_{rdq} \\ \phi_{rdq} &= l_{sr} \mathbf{i}_{sdq} + l_r \mathbf{i}_{rdq} \\ v_{s0} &= r_s i_{s0} + l_{ls} \frac{d}{dt} i_{s0} \\ v_{r0} &= r_r i_{r0} + l_{lr} \frac{d}{dt} i_{r0} \\ T_e &= P l_{sr} (i_{sq} i_{rd} - i_{sd} i_{rq}) \end{aligned}$$

where $\mathbf{v}_{sdq} = v_{sd} + jv_{sq}$, $\mathbf{i}_{sdq} = i_{sd} + ji_{sq}$, and $\phi_{sdq} = \phi_{sd} + j\phi_{sq}$ are the voltage, current, and flux dq vectors of the stator, respectively; v_{s0} and i_{s0} are the homopolar voltage and current of the stator, respectively (the equivalent rotor variables are obtained by replacing the subscript s by r); T_e is the electromagnetic torque; ω_r is the angular frequency of the rotor; r_s and r_r are

the stator and rotor resistances; l_s , l_{ls} , l_r , and l_{lr} are the self and leakage inductance of the stator and rotor, respectively; l_{sr} is the mutual inductance and P is the number of pole pairs of the machine. The dqo stator variables of the previous model can be determined from the abc variables by using the transformation given by

$$\mathbf{w}_{sdqo} = A_s \mathbf{w}_{abc}$$

with $\mathbf{w}_{sdqo} = [w_{sd} \ w_{sq} \ w_{so}]^T$, $\mathbf{w}_{abc} = [w_a \ w_b \ w_c]^T$ and

$$A_s = \sqrt{\frac{2}{3}} \begin{bmatrix} 1 & -\frac{1}{2} & -\frac{1}{2} \\ 0 & \frac{\sqrt{3}}{2} & -\frac{\sqrt{3}}{2} \\ \frac{\sqrt{2}}{2} & \frac{\sqrt{2}}{2} & \frac{\sqrt{2}}{2} \end{bmatrix}$$

Vectors \mathbf{w}_{sdqo} and \mathbf{w}_{abc} can be voltage or current or flux vectors and $A^{-1} s = A^T s$

IV. CONTROL STRATEGY

The proposed converter has the same objectives as in the conventional converter, as observed in Fig. 1(b), i.e., 1) dc-link voltage control, 2) power factor correction, and 3) three-phase voltage generation at the output-converter side. Additionally, the converter control of the

proposed system needs to control the circulating current. Fig. 3 presents the control block diagram for the proposed system. The capacitor dc-link voltages v_{C1} and v_{C3} are adjusted to their reference values v_{C1}^* and v_{C3}^* using controllers $RC1$ and $RC3$ (conventional PI-type controllers), respectively. Those controllers provide the amplitude of reference currents i_{a1}^*

and i_{3a}^* . To control power factor and harmonic content at the input-converter side, the instantaneous reference currents i_{1a}^* and i_{3a}^* are synchronized with the grid voltage, as given

in . The blocks $G - ig1$ and $G - ig3$ have two functions, i.e., synchronization with the grid (through a phase-locked loop scheme) and generation of the sinusoidal reference currents.

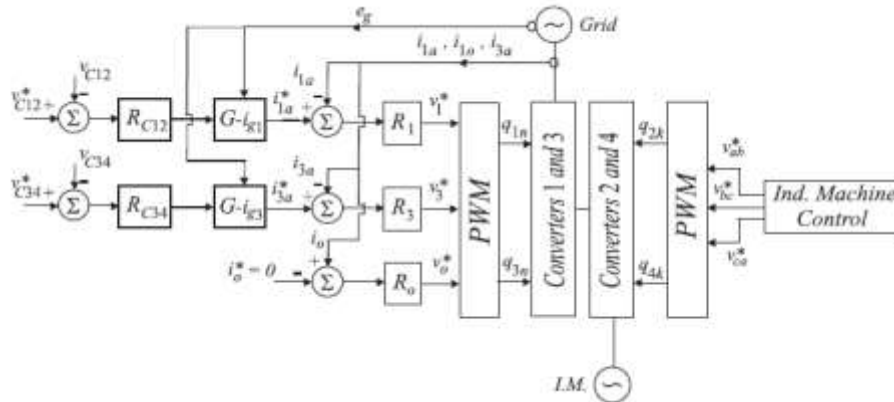


Fig. 3. Control block diagram..

V. FUZZY CONTROLLER MODEL

Fuzzy modeling is the method of describing the characteristics of a system using fuzzy inference rules. The method has a distinguishing feature in that it can express linguistically complex non-linear system. It is however, very hard to identify the rules and tune the membership functions of the reasoning. Fuzzy Controllers are normally built with fuzzy rules. These fuzzy rules are obtained either from domain experts or by observing the people who are currently doing the control. The membership functions for the fuzzy sets will be

derive from the information available from the domain experts and/or observed control actions. The building of such rules and membership functions require tuning. That is, performance of the controller must be measured and the membership functions and rules adjusted based upon the performance. This process will be time consuming. The basic configuration of Fuzzy logic control based as shown in Fig. 4.1 consists of four main parts i.e. (i) Fuzzification, (ii) knowledge base, (iii) Inference Engine and (iv) Defuzzification.

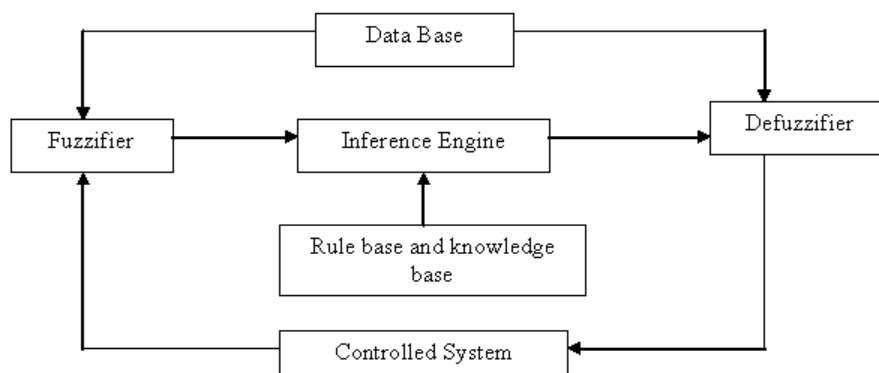


Fig.4 Structure of Fuzzy Logic controller

1 Fuzzification:

Fuzzification maps from the crisp input space to fuzzy sets in certain, input universe of discourse. So for a specific input value x , it is mapped to the degree of membership $\mu_A(x)$. The fuzzification involves the following functions. Measures the value of input variables.

1. Performs a scale mapping that transfers the range of values of input variables into corresponding universe of discourse.
2. Performs the function of fuzzification that converts input data into suitable linguistic variables, which may be viewed as labels of fuzzy sets.

The input variables to fuzzifier are the crisp controlled variables. Selection of the control variables relies on the nature of the system and its desired output. It is more common in the literature to use the output error and the derivative of output. Each of the fuzzy logic control (FLC) input and output signal is interpreted into a number of linguistic

variables. The number of linguistic variables specifies the quality of control which can be achieved using the fuzzy controller. As the number of linguistic variables increases, the computational time and required memory increases. Therefore a compromise between the quality of control and computational time is needed to choose the number is seven. Each linguistic variables NB, NM, NS, ZE, PS, PM, PB which stands for negative big, negative medium, negative small, zero positive small, positive medium, positive big respectively. For simplicity it is assumed that the membership functions are symmetrical and each one overlaps the adjacent functions by 50% i.e., triangle shaped function, the other type of functions used are trapezoidal-shaped and Bell-shaped. Figure 3.2 shows the seven linguistic variable and the triangular membership function with 50% overlap and the universe of discourse from $-a$ to a .

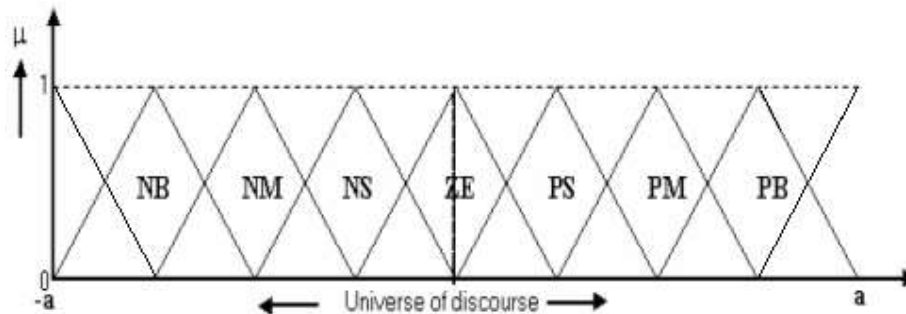


Fig 5 Triangular membership functions

2 Knowledge Base (KB):

Knowledge base comprises of the definitions of fuzzy MFs for the input and output variables and the necessary control rules, which specify the control action by using linguistic terms.

It consists of a database and linguistic control rule base.

1. The database provides necessary definitions, which are used to define linguistic control rules and fuzzy data, manipulation in a FLC.
2. The rule base characterizes the control goals and control policy of the domain experts by means of a set of a set of linguistic control rules.

3 Inference Mechanism:

The Decision – Making Logic Which plays an essential role and contains a set of fuzzy if-then rules such as

IF x is A and y is B then z is C

Where x , y and z are linguistic variables representing two input variables and one control output: A, B and C are linguistic values.

It is kernel of an FLC, it has the capability of simulating human decision making based on fuzzy control actions employing fuzzy implication and the rules of inference in fuzzy logic.

In general, fuzzy systems map input fuzzy sets to output fuzzy sets, fuzzy rules are the relation

between input/output fuzzy sets. They are usually in the form if A. (set of conditions are satisfied) then B, (set of consequences can be inferred). Each rule defines a fuzzy path in the Cartesian product $A \times B$ (system state space). The antecedents of each fuzzy rule describe a fuzzy input region in the state space. For a system of two-control variable with seven linguistic variables in each range, this leads to a 7x7 decision table. The knowledge required to generate the fuzzy rules can be derived from an off – line simulation, an expert operator and/or a design engineer. Some knowledge can be used on the understanding of the dynamic system under control. A lot of effort has been devoted to the creation of the fuzzy rules. Normally rule definition is based on the operator’s experience and the engineer’s knowledge. However, it has been noticed in practice that for monotonic systems a symmetrical rule table is very appropriate, although some times it may need slight adjustment based on behavior of the specific system. If the system dynamics are not known or if the system is highly non – linear, trial and error procedure and experience play an important role in defining the rules.

4 Defuzzification:

Defuzzification converts the linguistic variables to determine numerical values. Centroid method of defuzzification is used in this study.

- (1) A scale mapping, which converts the range of values of input variables into corresponding universe of discourse.
- (2) Defuzzification, which yields a non-fuzzy control action from an inferred fuzzy control action.

We defuzzify the output distribution B to produce a single numerical output, a single value in the output universe of discourse $Y = \{y_1, y_2, \dots, y_p\}$. The information in the output waveform B resides largely in the relative values of membership degrees. The simplest defuzzification scheme chooses that element Y_{max} . That has maximal membership put in the output fuzzy set B. $M_B (y_{max}) = \max m_B (y_j); 1 \leq j \leq k$

The maximum membership defuzzification scheme has two fundamental problems. First, the mode of the B distribution is not unique. In practice B is often highly asymmetric; even if it is unimodal infinitely many output distributions can share the same mode. The maximum membership scheme ignores the information in much of the waveform B. The natural alternative is the fuzzy centroid defuzzification scheme. The regions in which the control actions are overlapped depending upon their membership function. The area thus obtained is divided into narrow strips of equal width of each vertical line, the membership function and the corresponding point on the universe of discourse is evaluated. The centroid is calculated using the formula given below. The graphical representation of centroid is shown in Fig. below.

$$B = \frac{\sum_{j=1}^p Y_j \cdot m_B (y_j)}{\sum_{j=1}^p m_B (y_j)}$$

Where $m_B(y_j)$ = membership function of the j^{th} strip.
 y_j = Corresponding Crisp value of j^{th} strip. p = number of strips.

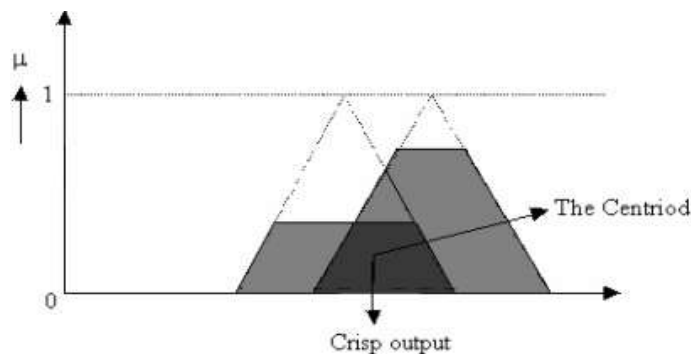


Fig 6 A graphical representation of Centroid

This value is actually the deterministic input required to regulate the process. The entire universe of discourse is then divided into seven triangles, equal in area, each representing the region of the linguistic variables as in fuzzification. The fuzzy centroid is

unique and uses all the information in the output distribution B. Computing the centroid is only step in the defuzzification process, which requires simple division.

VI. SIMULATION RESULTS

A). EXISTING RESULTS

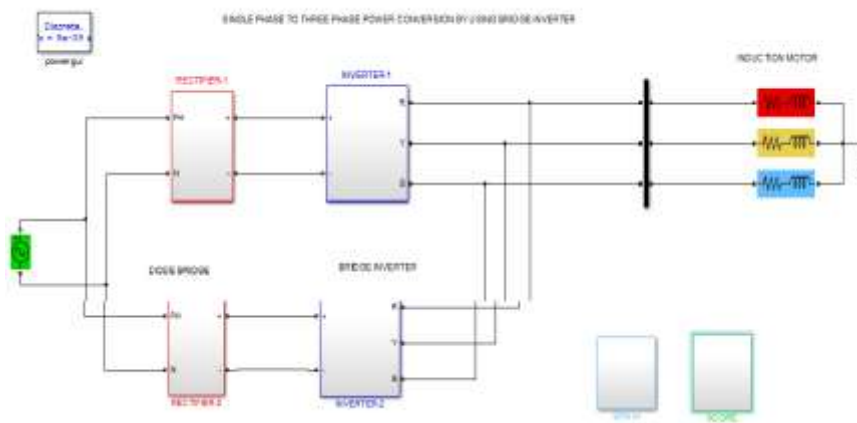


Fig 7. Circuit Diagram

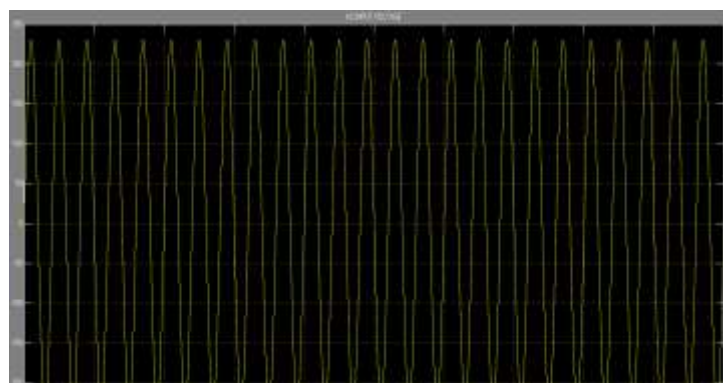


Fig 8. Input voltage

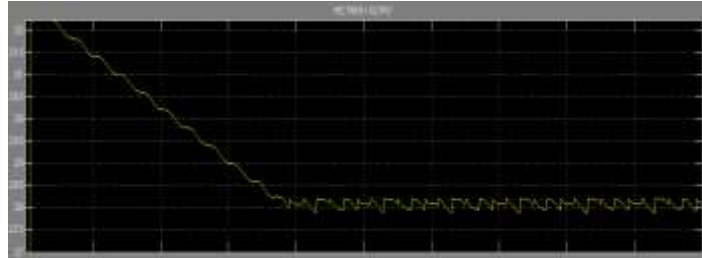


Fig 9. Rectifier Output

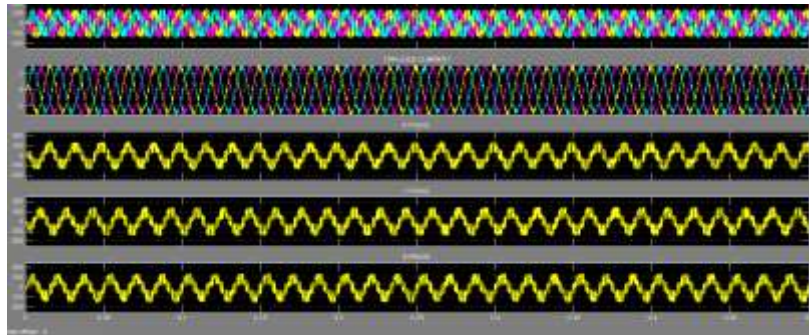


Fig 10. Total output with-out filter

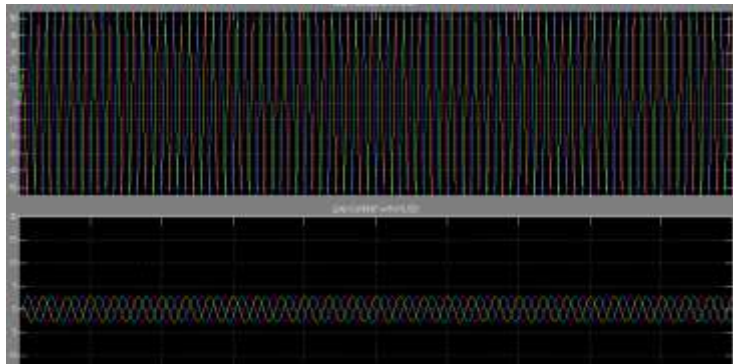


Fig 11. Total output with filter

B). EXTENSION RESULTS

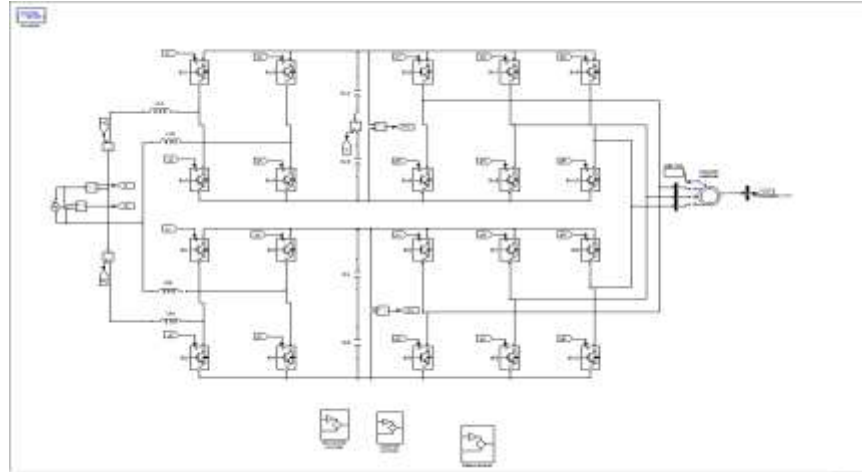


Fig 12. MATABL/SIMULINK diagram of proposed system

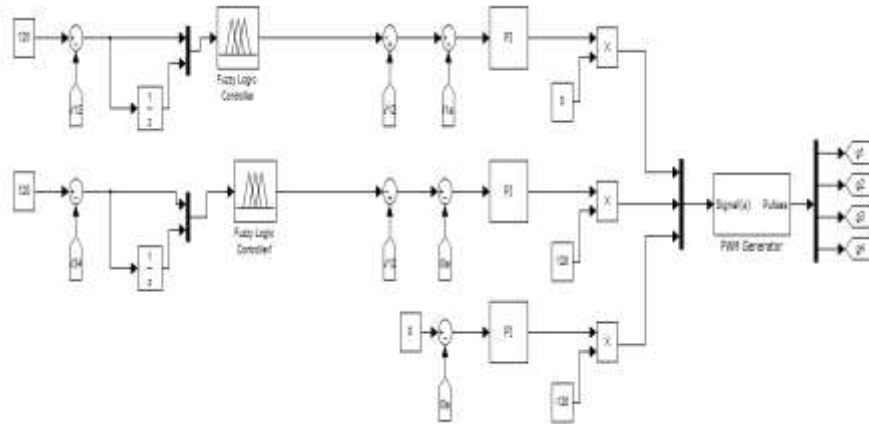


Fig 13. Source controller subsystem

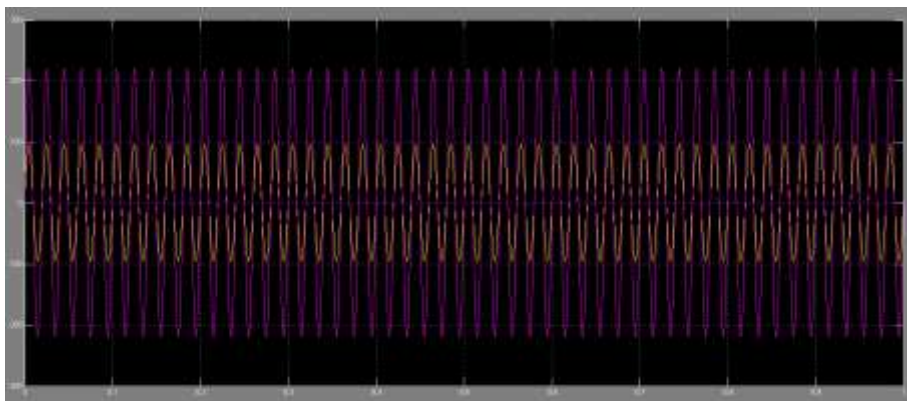


Fig 14. voltage and current of the grid,

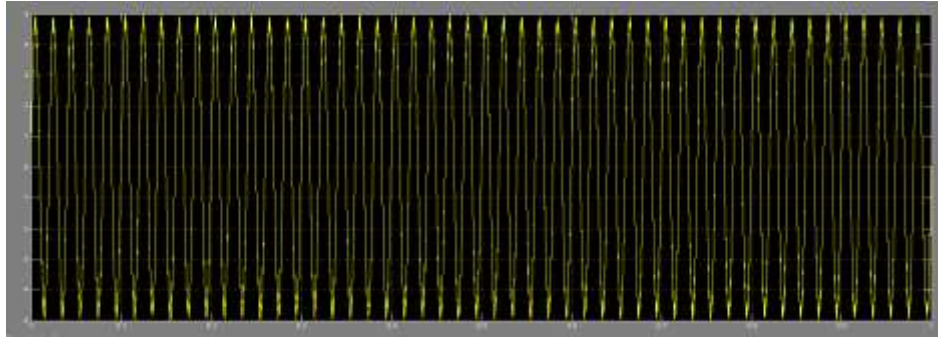


Fig 15. input current of the converter 1

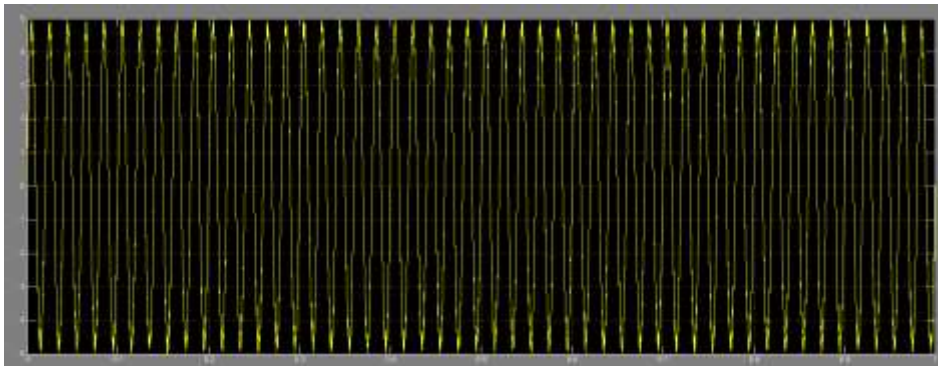


Fig 16. input current of the converter 2

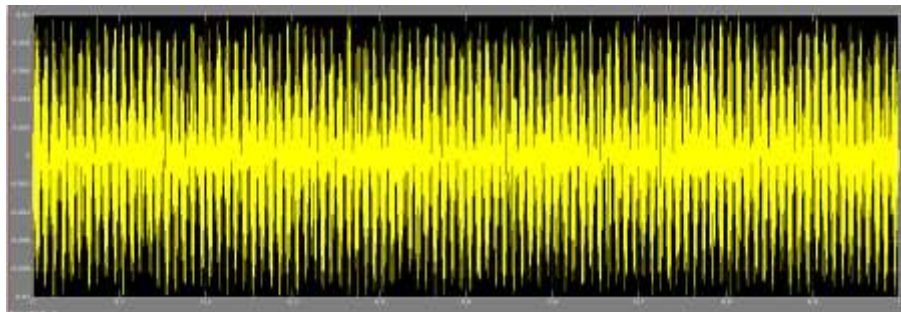


Fig 17. circulating current

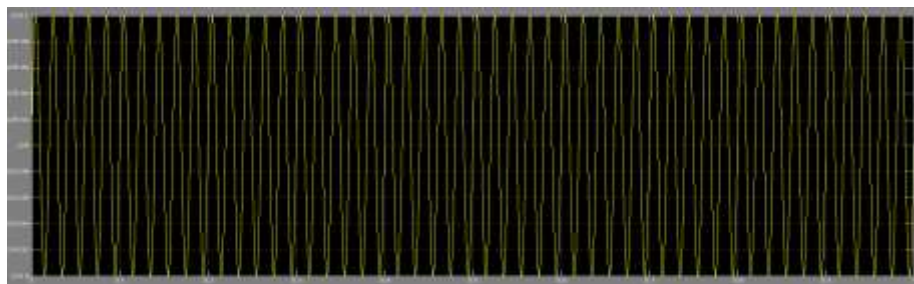


Fig 18. dc-link voltage in C12

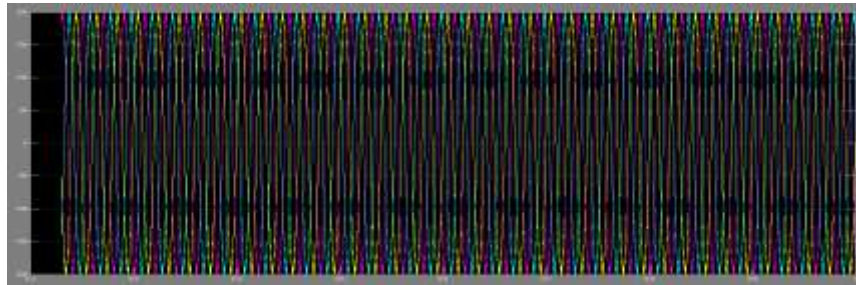


Fig 19. load currents

CONCLUSION

This project was proposed a single-phase to three-phase power conversion system with parallel rectifier and series inverter to cope with single-phase to three-phase asymmetry. Such converter guarantees both reduction in the input current processed by rectifier circuit and reduction of the output voltage processed by the inverter circuit. It is worth mentioning that, in spite of proposing a topology with features not yet observed on the technical literature, this paper presents a comprehensive model of the proposed converter, modulation strategy, and a general comparison with the conventional configuration. In extension we used fuzzy controller to controlling source side converter. And as well as it improve the wave shape and gives high accuracy compared to pid controller. Simulated results are also presented.

REFERENCES

- [1] A. H. Maggs, "Single-phase to three-phase conversion by the ferrarisarno system," *Electr. Eng.—Part I, General, J. Inst.*, vol. 93, no. 32, pp. 133–136, Aug. 1946.
- [2] K. Hisano, H. Kobayashi, and T. Kobayashi, "A new type single-phase to three-phase converter," *IEEE Trans. Magn.*, vol. 2, no. 3, pp. 643–647, Sep. 1966.

- [3] S. Dewan and M. Showleh, "A novel static single-to three-phase converter," *IEEE Trans. Magn.*, vol. 17, no. 6, pp. 3287–3289, Nov. 1981.

- [4] M. Liserre, "Dr. Bimal K. Bose: A reference for generations [editor's column]," *IEEE Ind. Electron. Mag.*, vol. 3, no. 2, pp. 2–5, Jun. 2009.

- [5] F. Blaabjerg, A. Consoli, J. A. Ferreira, and J. D. van Wyk, "The future of electronic power processing and conversion," *IEEE Trans. Ind. Appl.*, vol. 41, no. 1, pp. 3–8, Jan./Feb. 2005.

- [6] F. W. Gutzwiller, "Thyristors and rectifier diodes—the semiconductor workhorses," *IEEE Spectrum*, vol. 4, no. 8, pp. 102–111, Aug. 1967.

- [7] A. Elasser, M. H. Kheraluwala, M. Ghezzi, R. L. Steigerwald, N. A. Evers, J. Kretchmer, and T. P. Chow, "A comparative evaluation of new silicon carbide diodes and state-of-the-art silicon diodes for power electronic applications," *IEEE Trans. Indust. Appl.*, vol. 39, no. 4, pp. 915–921, Jul./Aug. 2003.

- [8] M.-K. Nguyen, Y.-G. Jung, and Y.-C. Lim, "Single-phase AC–AC converter based on quasi-z-source topology," *IEEE Trans. Power Electron.*, vol. 25, no. 8, pp. 2200–2210, Aug. 2010.

- [9] M.-K. Nguyen, Y. cheol Lim, and Y.-J. Kim, "A modified single-phase quasi-z-source AC–

AC converter,” IEEE Trans. Power Electron., vol. 27, no. 1, pp. 201–210, Jan. 2012.

[10] B. Saint, “Rural distribution system planning using smart grid technologies,” in Proc. Rural Electric Power Conf., Apr. 2009, pp. B3-1–B3-8.

[11] A. R. C. de Lima Montenegro Duarte, U. H. Bezerra, M. E. de Lima Tostes, and G. N. da Rocha Filho, “Alternative energy sources in the Amazon,” IEEE Power Energy Mag., vol. 5, no. 1, pp. 51–57, Jan./Feb. 2007.

[12] X. Wang, H. Zhong, Y. Yang, and X. Mu, “Study of a novel energy efficient single-phase induction motor with three series-connected windings and two capacitors,” IEEE Trans. Energy Convers., vol. 25, no. 2, pp. 433–440, Jun. 2010.

[13] M. Khan, I. Husain, and Y. Sozer, “Integrated electric motor drive and power electronics for bidirectional power flow between the electric vehicle and DC or AC grid,” IEEE Trans. Power Electron., vol. 28, no. 12, pp. 5774–5783, Dec. 2013.

[14] Y.-S. Lai, W.-T. Lee, Y.-K. Lin, and J.-F. Tsai, “Integrated inverter/ converter circuit and control technique of motor drives with dualmode control for EV/HEV applications,” IEEE Trans. Power Electron., vol. 29, no. 3, pp. 1358–1365, Mar. 2014.

[15] C. B. Jacobina, E. C. dos Santos, Jr, N. Rocha, and E. L. Lopes Fabricio, “Single-phase to three-phase drive system using two parallel single-phase rectifiers,” IEEE Trans. Power Electron., vol. 25, no. 5, pp. 1285–1295, May 2010.